Cyclin-dependent kinase 8/19 inhibition suppresses osteoclastogenesis by downregulating RANK and promotes osteoblast mineralization and cancellous bone healing.

Mehdi Amirhosseini, Magnus Bernhardsson, Pernilla Lång, Göran Andersson, Johan Flygare and Anna Fahlgren

Amirhosseini, M., Bernhardsson, M., Lång, P., Andersson, G., Flygare, J., Fahlgren, A., (2019), Cyclin-dependent kinase 8/19 inhibition suppresses osteoclastogenesis by downregulating RANK and promotes osteoblast mineralization and cancellous bone healing., *Journal of Cellular Physiology*. https://doi.org/10.1002/jcp.28321

Original publication available at:
https://doi.org/10.1002/jcp.28321

Cyclin-dependent kinase 8/19 inhibition suppresses osteoclastogenesis by downregulating RANK and promotes osteoblast mineralization and cancellous bone healing

Mehdi Amirhosseini[1], Magnus Bernhardsson[1], Pernilla Lång[2], Göran Andersson[2], Johan Flygare[3], Anna Fahlgren[1*]

1 Department of Clinical and Experimental Medicine, Faculty of Medicine and Health Sciences, Linköping University, Linköping, Sweden

2 Division of Pathology, Department of Laboratory Medicine, Karolinska Institutet, Karolinska University Hospital, Huddinge, Sweden.

3 Department of Molecular Medicine and Gene Therapy, Lund Stem Cell Center, Lund University, Lund, Sweden

*** Corresponding Author**: Anna Fahlgren

Department of Clinical and Experimental Medicine, Division of Cell Biology, Linköping University, 58185 Linköping, Sweden

Tel: +46 13 286710, **Fax**: +46 10 1034273, **E-mail**: anna.fahlgren@liu.se

Running Title: CDK8 inhibition prevents osteoclastogenesis

Keywords: **CDK8**; **Cyclin-dependent kinase 8**; **Osteoclasts**; **Osteoblasts; RANK**

Number of Figures: 7

Grants: Swedish Research Council (521-2013-2593, 2016-01822, 2016-06097, K2015-99x-10363-23-4)

Abstract

Cyclin-dependent kinase 8 (CDK8) is a Mediator complex-associated transcriptional regulator that acts depending on context and cell type. While primarily under investigation as potential cancer therapeutics, some inhibitors of CDK8 - and its paralog CDK19 - have been reported to affect the osteoblast lineage and bone formation. This study investigated effects of two selective CDK8/19 inhibitors on osteoclastogenesis and osteoblasts in vitro, and further evaluated how local treatment with a CDK8/19 inhibitor affects cancellous bone healing in rats. CDK8/19 inhibitors did not alter the proliferation of neither mouse bone marrow-derived macrophages (BMMs) nor primary mouse osteoblasts. RANKL-induced osteoclastogenesis from mouse BMMs was suppressed markedly by inhibition of CDK8/19, concomitant with reduced TRAP activity and CTX-I levels. This was accompanied by downregulation of PU.1, RANK, NFκB, NFATc1, DC-STAMP, TRAP and cathepsin K in RANKL-stimulated BMMs. Downregulating RANK and its downstream signaling in osteoclast precursors enforce CDK8/19 inhibitors as anti-catabolic agents to impede excessive osteoclastogenesis. In mouse primary osteoblasts, CDK8/19 inhibition did not affect differentiation but enhanced osteoblast mineralization by promoting ALP activity and downregulating osteopontin, a negative regulator of mineralization. In rat tibiae, a CDK8/19 inhibitor administered locally promoted cancellous bone regeneration. Our data indicate that inhibitors of CDK8/19 have the potential to develop into therapeutics to restrict osteolysis and enhance bone regeneration.

Keywords: CDK8; Cyclin-dependent kinase 8; Osteoclasts; Osteoblasts; RANK

Introduction

Osseointegration of orthopedic implants or bone regeneration during fracture healing depends on the delicate balance between the activity of the bone anabolic osteoblasts and bone degrading osteoclasts. Previous studies indicate that inhibitors of cyclin-dependent kinase 8 (CDK8), and its paralog CDK19, can affect bone tissue (Clarke et al., 2016; Ono et al., 2017). CDKs are a group of serine/threonine kinases that, besides controlling cell cycle progression, are involved in transcriptional regulation (Galbraith et al., 2010). CDK8, as part of the Mediator complex, is categorized as a transcriptional CDK. Although CDK8 is primarily known as a negative regulator of RNA polymerase II-dependent transcription, evidence supports that it can both activate or suppress transcription (Nemet et al., 2014; Rzymski et al., 2015; Szilagyi and Gustafsson, 2013). It appears that CDK8 acts as a context-related regulator of gene expression. CDK8 has been implicated to play diverse roles in different signaling pathways like Wnt/β-catenin signaling (Firestein et al., 2008; Morris et al., 2008), TGF-β/BMP signaling (Alarcon et al., 2009), and Notch signaling (Fryer et al., 2004) among others. CDK inhibitors have been proposed as potential therapeutics to treat cancer mainly due to their ability to inhibit cell cycle progression (Law et al., 2015). Several CDK8 inhibitors have shown the ability to suppress tumor growth through both cell cycle block and transcriptional regulation (Pelish et al., 2015; Rzymski et al., 2015).

Previous studies on effects of CDK8/19 inhibitors on bone tissue were restricted to their effects on bone formation (Clarke et al., 2016) and osteoblast differentiation (Ono et al., 2017), while there are no reports on how inhibition of CDK8 affects osteoclast differentiation. CDK8 is involved in the process of switch from proliferation to differentiation (Szilagyi and Gustafsson, 2013). It induces transcription of p21 (Szilagyi and Gustafsson, 2013), which together with p27 and p57 belong to the Cip/Kip family of CDK inhibitors that cause cell cycle withdrawal (Vidal and Koff, 2000). Cell cycle withdrawal in

osteoclast precursors is reported to be necessary for osteoclast formation (Kwon et al., 2016; Mizoguchi et al., 2009).

Receptor activator of nuclear factor κ-B (NFκB) ligand (RANKL), is the crucial factor for osteoclast differentiation. It activates NFκB, a transcription factor for osteoclast differentiation. NFκB in turn induces nuclear factor of activated T-cells 1 (NFATc1), known as the master transcription factor for osteoclast differentiation, which prompts osteoclastogenesis (Boyce et al., 2015; Ono and Nakashima, 2018). RANKL is also suggested to have anti-proliferative properties leading to cell cycle arrest during osteoclastogenesis (Bharti et al., 2004; Sankar et al., 2004). Modulating CDK8 may advantageously be used to restrain osteoclast differentiation in pathologic conditions with excessive bone resorption. In this study, we aimed to investigate (1) effects of CDK8 inhibition on osteoclastogenesis and primary osteoblast differentiation and function in vitro, and (2) effects of local treatment with a CDK8 inhibitor on healing of cancellous bone injury in a rat model for bone regeneration.

Materials and Methods

CDK8/19 inhibitors

Two selective inhibitors of CDK8/19, Senexin B and 15w, were used in this study. Senexin B (SNX2-1-165) is a potent, selective CDK8/19 inhibitor with IC50 values ranging from 24-50 nM (McDermott et al., 2017; Ronnison, 2014). Senexin B was synthesized to 96% purity (UV254/290nm) by Keytolead AB (Södertälje, Sweden). To confirm that our findings are due to inhibition of CDK8/19, we included a second potent and highly selective CDK8/19 inhibitor, 15w, identified in our laboratory (Patent WO2017076968A1). Kinase selectivity

profiling, using DiscoverX for KinomeScan scanELECT®platform, has confirmed that 15w is a selective inhibitor of CDK8/19 (Table S1).

Animals

Thirty-four 10-12-week-old male C57bl/6 mice were used for in vitro osteoclast and osteoblast differentiation assays (ethical # 4-15). Thirty 10-12-week-old male Sprague-Dawley rats (425 g; SD = 19) were used for evaluating effects of local administration of Senexin B in a cancellous bone healing model (ethical # 1605). Animals were housed in pathogen-free ventilated cages with a 12-hour light-dark cycle with free access to food and water. All experiments were carried out according to guidelines for care and treatment of experimental animals recommended by the animal experiments ethical committee in Linköping and the EU Directive 2010/63/EU.

Isolation of mouse bone marrow macrophages

Mice were euthanized using CO_2 gas. Tibiae and femora were collected. Soft tissue was removed, and the proximal end of the tibiae was cut. Bone marrow was extracted by centrifugation of the bones at 3,500 g for 5 minutes (Amend et al., 2016). The isolated bone marrow cells were seeded in 100-mm non-treated plastic petri-dishes in α-MEM (Gibco, Paisley, UK) supplemented with 10% heat-inactivated Fetal Bovine Serum (FBS) (Hyclone, Logan, UT), 1% Penicillin-Streptomycin-Fungizone (PSF) (Gibco), and 100 ng/mL recombinant mouse macrophage colony stimulating factor (M-CSF) (R&D Systems, Abingdon, UK) for 72 hours at 37 °C with 5% CO_2. The non-adherent cells were then washed away with Ca^{2+}- and Mg^{2+}-free PBS and the bone marrow macrophages (BMMs)

were harvested using 0.02% EDTA (Sigma Aldrich; St Louis, MO) and used for osteoclast differentiation and resorption assays.

Isolation of mouse primary osteoblasts

After removal of soft tissue and bone marrow, mouse tibiae and femora were minced into 1-mm pieces and treated with 2 mg/mL collagenase type 2 (Worthington Biochemical, Lakewood, NJ) in DMEM (low glucose) (Gibco) for 2 hours at 37 °C. Bone pieces were then washed in DMEM and placed in 25 Cm^2 flasks in DMEM supplemented with 10% FBS (Hyclone),1% PSF (Gibco), and 100 µg/mL ascorbic acid (Acros Organics). Medium was refreshed every 2 days. When subconfluent, osteoblasts were harvested using 0.25% trypsin solution (Gibco), passaged once (P1), and used for the experiments (Bakker and Klein-Nulend, 2012).

Toxicity assay

Lactate dehydrogenase (LDH) release from cells was measured as a marker for cytotoxicity using CytoTox 96® Non-Radioactive Cytotoxicity Assay Kit (Promega, Madison, WI). 10,000 mouse BMMs in 96-well plates were cultured in α-MEM with 10% FBS, 1% PSF and 50 ng/mL M-CSF. Mouse primary osteoblasts at 2,500 cells/well were cultured in DMEM with 10% FBS and 1% PSF in 96-well plates. At the start of the culture, BMMs and osteoblasts were treated with 1 and 1.5 µM of the CDK8/19 inhibitors for 24 hours. 50 µL of the culture supernatant was then mixed with 50 µL of CytoTox 96® Reagent in 96-well plates and incubated for 30 minutes in room temperature. Next, 50 µL of stop solution was added to the wells and the absorbance was measured at 490 nm using Spark™ 10M microplate reader

(Tecan). The experiments were performed using cells from six mice analyzed separately (n = 6) in duplicates.

Proliferation assay

To assess the effect of CDK8/19 inhibitors on proliferation, the BrdU Cell Proliferation ELISA kit (Roche Diagnostics GmbH, Mannheim, Germany) was used. Mouse BMMs at 10,000 cells/well in α-MEM, and primary osteoblasts at 2,500 cells/well in DMEM were seeded in 96-well plates. After 24 hours of serum depletion and synchronization, medium was changed and BMMs were cultured in α-MEM with 10% FBS, 1% PSF and 50 ng/mL M-CSF, and osteoblasts were cultured in DMEM supplemented with 10% FBS and 1% PSF for an additional 8 hours with or without 1 and 1.5 µM of the CDK8/19 inhibitors. During the 8 hours the cells were labeled with Bromodeoxyuridine (BrdU) solution at a final concentration of 10 µM to measure newly synthesized DNA according to the manufacturer's instructions. The culture medium containing labeling solution was removed and the cells were fixed, and DNA was denatured. Next, anti-BrdU-POD solution was added followed by 90 minutes of incubation in room temperature. After three washing steps, TMB (Tetramethyl-benzidine) substrate solution was added with 20 minutes of incubation. After adding the stop solution (1 M H_2SO_4) to the wells, absorbance was measured at 450 nm (reference wavelength: 690 nm). The experiments were performed using cells from six mice analyzed separately (n = 6) in duplicates.

Osteoclast culture

Mouse BMMs were seeded at 10,000 cells/well in 96-well plates with or without 0.5, 1 and 1.5 µM of the CDK8/19 inhibitors in α-MEM with 10% FBS and 1% PSF. 50 ng/mL M-CSF

(R&D Systems) and 10 ng/mL recombinant mouse RANKL (R&D Systems) were added to the culture to support osteoclast differentiation. Medium was refreshed on day 2. On day 4, cells were fixed with 4% formaldehyde solution and stained for tartrate-resistant acid phosphatase (TRAP) using an Acid Phosphatase, Leukocyte Kit (Sigma). (Kim et al., 2010). The experiments were performed using cells from seven mice analyzed separately (n = 7) in triplicates. TRAP-positive cells with at least three nuclei were counted, under a light microscope, as osteoclasts in the whole surface area of 96-well plates.

TRAP activity, CTX-I ELISA, and pit assay

Mouse BMMs were seeded at 15,000 cells/well in 96-well plates on the surface of 4x4-mm bovine bone slices (200 µm in thickness) with or without 1 µM of the CDK8/19 inhibitors in α-MEM with 10% FBS, 1% PSF as well as 50 ng/mL M-CSF and 10 ng/mL RANKL. The medium was refreshed every 2 days. Culture supernatants from days 10-12 of the culture were collected to evaluate TRAP enzyme activity and C-terminal telopeptide of type I collagen (CTX-I) levels.

Using p-nitrophenylphosphate (pNPP) as substrate, activity of TRAP in the culture supernatant, corresponding to p-nitrophenol levels released from pNPP (µmol/min/µL media), was determined as described previously (Lång and Andersson, 2005). The released p-nitrophenol was converted into p-nitrophenolate by the addition of 0.9 M NaOH. The absorbance was measured at 405 nm.

CrossLaps® for Culture CTX-I ELISA kit (IDS, Boldon, UK) was used to check how CTX-I levels, a marker for bone resorption, were affected by inhibition of CDK8. Briefly, samples (diluted three-fold) and an antibody solution, consisting of biotinylated monoclonal anti-CTX-I and peroxidase-conjugated anti-CTX-I antibody, were added to the streptavidin pre-

coated wells and incubated for 2 hours at room temperature on shaker. After five washing steps, the wells were incubated for 15 minutes with TMB substrate solution. Next, the stop solution was added, and absorbance was measured at 450 nm (reference wavelength: 650 nm).

On day 12, the bone slices were washed with distilled water and sonicated for 30 minutes in cold NH_4OH. After twice washed in water, the bone slices were incubated for 10 minutes in a saturated solution of potassium aluminum sulfate dodecahydrate ($KAl(SO_4)2*12H_2O$) and washed twice in water again. The bone slices were then stained with Coomassie brilliant blue solution. Resorption pits on bovine bone slices were analyzed by taking pictures covering approximately 70% of the surface of the bone slice. This was the same area and position, adjusted by the center of the 4x4-mm bone slices, for all samples. The resorbed surface area, stained by Coomassie brilliant blue, was quantified using the ImageJ analysis software. The experiments (TRAP activity, CTX-I ELISA, and pit assay) were performed using cells from three mice analyzed separately (n = 3) in duplicates.

Western blot for NFATc1

Mouse BMMs were cultured, in 24-well plates at 60,000/well, in α-MEM with 10% FBS, 1% PSF as well as 50 ng/mL M-CSF and 10 ng/mL RANKL with or without 1 μM of the CDK8/19 inhibitors for 48 hours. The wells were washed with PBS and cells were lyzed using RIPA buffer (Cell Signaling Technology, Danvers, MA) containing 1 mM Phenylmethylsulfonyl fluoride (PMSF). Protein, concentrated using Nanosep 10K Omega (PALL, Port Washington, NY), was loaded onto Mini-Protean TGX gels (Bio-Rad Laboratories, Hercules, CA) and run and transferred as previously described (Patlaka et al., 2014). Primary antibody diluted 1:1,000 in TBS-T, was rabbit anti-human NFATc1 (Abcam,

Cambridge, UK, Cat# ab25916, RRID: AB_448901). Membranes were washed in TBS-T for 15 minutes and then stained with secondary antibody, IRDye 800CW donkey anti-rabbit (LI-COR Biosciences Ltd, Cambridge, UK) diluted 1:15,000 in TBS-T, for 30 minutes at room temperature before washed in TBS-T for 45 minutes. Membranes were documented and analyzed using Odyssey Fc (LI-COR) equipped with software Image Software (LI-COR). NFATc1 (101 kDa isoform) signal was calculated as the signal normalized to total protein loaded onto the TGX gel. The experiment was performed using cells from six mice analyzed separately (n = 6).

Alkaline phosphatase activity and mineralization assay

Mouse primary osteoblasts were seeded at 8,000 cells/well with or without 1 and 1.5 μM of the CDK8/19 inhibitors in 48-well plates. Osteoblast differentiation medium consisted of DMEM with 10% FBS and 1% PSF supplemented with 50 μg/mL ascorbic acid (Acros Organics) and 10 mM β-glycerophosphate (Sigma). Medium was changed every 2 days (Watanabe et al., 2017). Cells were lyzed in distilled water on day 10 and alkaline phosphatase (ALP) activity was evaluated in the supernatant based on release of p-nitrophenol from pNPP substrate using an ALP colorimetric assay kit (Abcam) according to manufacturer's instructions. The absorbance was measured at 405 nm. On day 18, the cell layer was decalcified for 24 hours in 0.6 M HCl at room temperature and the calcium content was measured in the supernatant by Arsenazo III colorimetric method (Randox Laboratories, Crumlin, UK) (Haarhaus et al., 2013). Briefly, 200 μL of Arsenazo III solution was added to 3 μL of the supernatant in 96-well plates and calcium levels were determined at 650 nm. The experiments were performed using cells from five mice analyzed separately (n = 5) in

duplicates. ALP activity and calcium content measurements were normalized to the total protein levels in the cell layer determined by BCA protein assay kit (Pierce, Rockford, IL).

RNA isolation and real-time quantitative PCR

Mouse BMMs in presence of M-CSF (50 ng/mL) and RANKL (10 ng/mL) were cultured with or without 1 μM of the CDK8/19 inhibitors. Similarly, primary osteoblasts were cultured in osteoblast differentiation medium with or without 1 μM of the inhibitors. Using TRIzol (Invitrogen), BMMs were lyzed after 8 and 48 hours and osteoblasts were lyzed after 24 and 72 hours. RNA was extracted by a combination of TRIzol and RNeasy Mini Kit (Qiagen, Sollentuna, Sweden) methods (Reno et al., 1997). Concentration and quality of RNA were checked by Nanodrop ND-1000 (NanoDrop Technologies, Wilmington, DE). RNA samples were converted to cDNA using High Capacity cDNA Reverse Transcription Kit (Applied Biosystems, UK). Primers (Applied Biosystems) for NFATc1 (Mm00479445_m1), NFκB2 (Mm00479807_m1), RANK (Mm00437132_m1), PU.1 (Mm00488140_m1), DC-STAMP (Mm04209236_m1), TRAP (Acp5) (Mm00475698_m1), Cathepsin K (Ctsk) (Mm00484039_m1), p27 (Mm00495994_m1), p21 (Mm04205640_g1), β-catenin (Mm00483039_m1), Runx2 (Mm00501584_m1), Osterix (Sp7) (Mm04209856_m1), ALP (Alpl) (Mm00475834_m1), Col1a1 (Mm00801666_g1), Osteopontin (Spp1) (Mm00436767_m1), Bone sialoprotein (iBsp) (Mm00492555_m1), Stat1 (Mm01257286_m1), Stat5a (Mm03053818_s1), Stat5b (Mm00839889_m1), RANKL (Mm00441906_m1), and Osteoprotegerin (OPG) (Mm00435454_m1) were used and qPCR reaction was performed using TaqMan Fast PCR Master mix (Applied Biosystems) by standard curve methodology. The experiments were performed using cells from six mice analyzed separately (n = 6) in duplicates. mRNA expression levels in BMMs and osteoblasts

were normalized to geometric mean of beta-actin (Mm02619580_g1) and beta-2 microglobulin (Mm00437762_m1), and to beta-actin respectively.

Total Stat1 and p-Stat1 (S727) ELISA

Mouse primary osteoblasts were seeded at 8,000/well in 48-well plates in osteoblast differentiation medium with or without 1 µM of the CDK8/19 inhibitors for 1 hour to check phosphorylation of Stat1 at Serine 727, and for 72 hours to check total Stat1 levels. The cells were lyzed using RIPA buffer (Cell Signaling Technology). Stat1 (pS727) + Total Stat1 ELISA Kit (Abcam) was used according to the manufacturer's instructions. Briefly, cell lysate samples were added to pre-coated wells with anti-phospho-Stat1 (Ser727) or anti-Stat1 antibody and incubated for 2.5 hours. The wells were washed, and biotinylated Stat1 antibody was added for 1 hour. After washing the wells, the HRP-Streptavidin solution was added followed by 1 hour of incubation and washing the wells. The wells were incubated with TMB substrate solution for 30 minutes and then the stop solution was added. The absorbance was measured at 450 nm. All incubation steps were performed at room temperature on shaker. Phosphorylated Stat1 (S727) levels were normalized to total Stat1 levels both measured in samples harvested after 1 hour of treatment with the CDK8/19 inhibitors. Total Stat1 levels were normalized to total protein levels in the cell lysates measured using BCA protein assay kit (Pierce). The experiments were performed using cells from six mice analyzed separately (n = 6) in duplicates.

Local administration of a CDK8/19 inhibitor into rat cancellous bone

To further evaluate the effect of CDK8 inhibition on the skeleton, we used a rat model in which we previously found that locally administered anti-resorptive bisphosphonates

enhanced bone mass (Wermelin et al., 2008). Senexin B, with documented in vivo activity (McDermott et al., 2017), was chosen for evaluating the effect of CDK8 inhibition on bone regeneration. 1 µg of Senexin B or vehicle (DMSO) (n = 15/group) were administered inside a drill hole made on the tibiae of Sprague-Dawley rats. The complete procedure has been described elsewhere (Bernhardsson et al., 2015). Briefly, the skin and muscle were incised to expose the bone surface. 1.2 mm drill holes were made in the antero-medial aspect of the proximal metaphysis on the tibiae, about 2 mm below the growth plate. To deliver the inhibitor, it was added into a fibrin scaffold. The fibrin scaffold consisted of 4 mg/ml human fibrinogen and 1 unit of human thrombin (Sigma) (Herchenhan et al., 2015). A Senexin B stock dissolved in DMSO (as vehicle) was diluted to the desired concentration in PBS and mixed in the fibrinogen solution prior to addition of thrombin. The fibrin scaffolds were then inserted into the hole in the tibiae. Control animals were administered corresponding amounts of DMSO dissolved in the scaffolds. After 14 days, the rats were sacrificed using CO_2 gas and the tibiae were collected.

Micro-computed tomography (Micro-CT)

The tibiae were fixed in 4% paraformaldehyde for 24 hours before being scanned in a micro-CT (Skyscan 1174, v. 2; Bruker, Aarteselaar, Belgium). Radiographic images of the tibiae were acquired using a pixel size of 11.2 µm, 0.5 mm aluminum filter, rotation step of 0.4°, frame field averaging of 3 and energy settings of 50 kV and 800 µA in a 180° scan. Using NRecon (Skyscan, v. 1.6.8.0; Aarteselaar, Belgium), the images were reconstructed, and corrected for ring artifacts and beam hardening. In the reconstructed drill holes, starting from the endosteum and extending into the marrow compartment, a volume of interest (VOI) defined as a cylinder with a diameter of 1.1 mm and 1.5 mm in length was constructed. To

calibrate the bone mineral density (BMD) in the VOIs, 2 hydroxyapatite standards (0.25 and 0.75 g/cm3) were used before the total bone volume (BV/TV) could be measured in CTAn (Skyscan, v. 1.10; Aarteselaar).

Statistics

Kruskal-Wallis ANOVA was used to examine differences between all the groups (Control, Senexin B, 15w). Differences induced by each CDK8/19 inhibitor compared to controls were then determined by Mann-Whitney *U* test using GraphPad Prism (version 7.03; GraphPad Software Inc., San Diego, CA). A p-value ≤ 0.05 was considered statistically significant.

Results

CDK8/19 inhibitors showed no cytotoxic effects on BMMs or osteoblasts

Treatment with 1 and 1.5 µM of Senexin B and 15w for 24 hours had no significant effects on LDH release rate from BMMs and osteoblasts compared to controls (Fig. 1A, B) indicating that CDK8/19 inhibitors did not display cytotoxic effects at these concentrations. DMSO at corresponding concentrations used with the inhibitors showed no effects on LDH release (Fig. S1A, B).

Proliferation rate of BMMs and osteoblasts was not affected by CDK8/19 inhibition

After 8 hours of treatment with 1 and 1.5 µM of Senexin B and 15w, proliferation rate of mouse BMMs, as osteoclast precursors, and primary osteoblasts showed no difference compared to controls (Fig. 1C, D). DMSO with corresponding concentration had no effects

on proliferation rate (Fig. S1C, D). The lack of effect on proliferation rate of BMMs and osteoblasts by CDK8/19 inhibitors was also observed in proliferation assay with longer labeling time (EdU labeling of BMMs for 48 hours and osteoblasts for 72 hours) (data not shown).

CDK8/19 inhibition suppressed osteoclast differentiation from mouse BMMs in vitro

Treatment of mouse BMMs with 1 and 1.5 µM Senexin B and 15w suppressed osteoclast differentiation substantially compared to controls (82% and 90% decrease by 1.5 µM of Senexin B and 15w respectively). 15w reduced the number of osteoclasts significantly already at 0.5 µM (Fig. 2A-C). 1 µM of Senexin B and 15w significantly decreased both TRAP activity (68% and 83% respectively) and CTX-I levels (38% and 74% respectively) in the supernatant collected from the culture of BMMs on bovine bone slices (days 10-12) (Fig. 2D, E). Similarly, pit assay showed that resorbed area on bovine bone slices was significantly decreased by 1 µM of both CDK8/19 inhibitors (Fig. 2F, G). We observed a 14% reduction in resorbed area with DMSO (Fig. S1E); however, the decrease in resorbed area by Senexin B (40%) and 15w (57%) compared to controls was more pronounced. DMSO, at corresponding concentrations had no significant effects on osteoclast numbers, TRAP activity or CTX-I levels (Fig. S1F-H).

We further tested how withdrawing the CDK8/19 inhibitors from osteoclast differentiation assay will affect osteoclast numbers and resorbed area, i.e. whether the effects were reversible or not. To this end, we performed osteoclast culture for a longer time period (7 days), to ensure that we could detect a possible reversal of osteoclast suppression by withdrawing the inhibitors. Treating BMMs with 1 µM of Senexin B and 15w for only the first 48 hours of the 7-day culture was sufficient for suppressing osteoclast differentiation

significantly (Fig. S2A). When BMMs, cultured on bovine bone slices, were treated with 1 μM of CDK8/19 inhibitors for only the first 48 hours of the culture (total culture time: 12 days), a slight decrease in resorbed area was observed (Fig. S2B). To further examine the effects of CDK8/19 inhibition on osteoclastogenesis during early or late stages of differentiation, BMMs were treated with the CDK8/19 inhibitors (0.5, 1 and 1.5 μM) either for the whole culture period (0-96 hours), or only once at the start of the culture (0-48 hours), or only in the later stage of the culture (48-96 hours) while medium was refreshed at 48 hours for all cultures. Inhibition of CDK8 for only the early stages of the osteoclast culture (0-48 hours) showed a slightly more suppressive effect on osteoclast differentiation compared to treatment in the later stages of the culture (48-96 hours), while inhibition of CDK8 for the whole 96 hours had the greatest effect on osteoclast numbers (Fig. S3A-C).

At mRNA level, treatment of BMMs with 1 μM of CDK8/19 inhibitors for 48 hours showed suppressive effects on expression of genes promoting osteoclastogenesis. PU.1 mRNA was significantly downregulated by 15w while the decrease in PU.1 mRNA level caused by Senexin B (24%) did not reach statistical significance (Fig. 3A). RANK, NFκB, NFATc1 and dendritic cell-specific transmembrane protein (DC-STAMP) mRNA were downregulated significantly by both Senexin B and 15w in BMMs (Fig. 3B-E). mRNA expression of the osteoclast markers TRAP and cathepsin K at 48 hours was significantly downregulated by 15w. The tendency to downregulation of TRAP and cathepsin K mRNA levels (38% and 35% respectively) induced by Senexin B at 48 hours was not statistically significant (Fig. 3F, G).

mRNA levels were assessed at 8 hours in order to detect possible early regulation of β-catenin, p27, p21, and Stat1, Stat5a and Stat5b by CDK8/19 inhibition. β-catenin mRNA expression in BMMs was significantly upregulated by both inhibitors at both 8 and 48 hours (Fig. 3H). Downregulation of p27 mRNA was detected at both 8 and 48 hours by both

inhibitors compared to controls (Fig. 3I), while p21 expression was not regulated at either time points (Fig. 3J). No significant changes in Stat1 mRNA expression at 8 or 48 hours were detected (Fig. 3K). Stat5a and Stat5b mRNA were downregulated at 48 hours by both CDK8/19 inhibitors (Fig. 3L, M).

Protein levels of NFATc1 were also significantly decreased by 1 µM of Senexin B (58%) and 15w (68%) after 48 hours compared to controls in BMMs (Fig. 3N) confirming that changes observed at mRNA level correspond to expression of NFATc1 protein.

Inhibition of CDK8/19 enhanced alkaline phosphatase activity and calcium deposition by mouse primary osteoblasts

1.5 µM of Senexin B increased ALP activity in mouse primary osteoblasts significantly compared to controls (Fig. 4A). The rise in ALP activity induced by 15w (5-fold) was not statistically significant (Fig. 4B). The increase in calcium deposition induced by Senexin B compared to controls (5-fold) was not statistically significant (Fig. 4C). 15w, at 1 and 1.5 µM, significantly enhanced calcium deposition by osteoblasts compared to controls (Fig. 4D). Corresponding concentrations of DMSO showed no significant effects on ALP activity or calcium deposition (Fig. S1I, J).

mRNA expression of Runx2 and Osterix, two major transcription factors for osteoblast differentiation, as well as ALP, collagen, type I, alpha 1 (Col1a1) and bone sialoprotein as markers for osteoblast differentiation were not significantly regulated by 1 µM of either of the CDK8/19 inhibitors at 24 or 72 hours (Fig. 5A-E). Similarly, expression of β-catenin showed no significant changes (Fig. 5F). Osteopontin, however, was significantly downregulated by both inhibitors at 72 hours (Fig. 5G). Expression of p21 and p27 mRNA were not significantly changed by either of the CDK8/19 inhibitors (Fig. 5H, I). No

significant changes in mRNA expression of RANKL, OPG or the RANKL/OPG ratio was detected following CDK8/19 inhibition (Fig. 5J-L).

A significant downregulation in Stat1, Stat5a and Stat5b mRNA was induced by both inhibitors at 72 hours (Fig. 5M-O). While phosphorylation of Stat1 at Serine 727 was not affected by 1 µM of CDK8/19 inhibitors after one hour in osteoblasts (Fig. S4A), total Stat1 protein levels after 72 hours were significantly decreased (Fig. S4B).

Local treatment with a CDK8 inhibitor increased bone mass and bone mineral density

To determine in vivo effects of CDK8 inhibition, Senexin B was locally administered to the bone tissue using a model with a drill hole defect. Local treatment with 1 µg of Senexin B, in a fibrin scaffold, significantly increased BV/TV (28%) and BMD (45%) in rat tibiae after 14 days compared to vehicle-treated animals (Fig. 6A-C).

Discussion

Previous reports on effects of CDK8 inhibition on bone tissue are limited to osteoblasts and bone formation. In this study, we demonstrate for the first time that (1) inhibition of CDK8 suppressed osteoclast differentiation from mouse bone marrow macrophages in vitro, and (2) local administration of a CDK8 inhibitor, Senexin B, increased bone volume fraction and bone mineral density in a rat model for cancellous bone healing. We further report that CDK8 inhibition promoted mineralization by primary mouse osteoblasts probably through downregulation of osteopontin and increased ALP activity (Fig. 7).

Together with Cyclin C, the kinases CDK8 or CDK19 form a regulatory component of the Mediator complex. The mediator kinase substrates are likely cell- and context-dependent but

have been reported to include Stat1 and other transcription factors (Poss et al., 2016). CDKs are well known regulators of cell cycle progression. Ample evidence supports a role for p21 and p27, two endogenous cyclin-dependent kinase inhibitors, in osteoclast differentiation. Induction of p27 alone (Mizoguchi et al., 2009), or p27 together with p21 (Okahashi et al., 2001; Sankar et al., 2004) have been shown to regulate RANKL-induced osteoclast differentiation. This regulatory role of p27 and p21 in osteoclastogenesis is attributed to their ability to induce cell cycle arrest. It is shown that cells deficient in p27 are inefficient in cell cycle withdrawal in response to RANKL (Sankar et al., 2004). A previous study (Mizoguchi et al., 2009) demonstrated that mRNA and protein levels of p27, rather than p21, are elevated by RANKL in BMMs. In our study, both CDK8 inhibitors downregulated p27 mRNA in BMMs. This corroborates the role of p27 in osteoclast differentiation. However, proliferation rate of BMMs treated with CDK8 inhibitors showed no difference compared to controls. This can be explained by the fact that inhibition of CDK8 leading to p27 downregulation, can abrogate the RANKL-induced cell cycle withdrawal that is necessary for osteoclastogenesis; thus, the osteoclast differentiation was suppressed by the inhibitors while no difference in proliferation rate was detected.

Downregulation of RANK mRNA in BMMs suggests CDK8/19 inhibitors to be capable of blunting signaling pathways downstream of RANK-RANKL axis, including NFκB and NFATc1, and suppress osteoclastogenesis with direct effect on osteoclast precursors. The transcription factor PU.1 plays essential role in osteoclast differentiation through regulation of RANK (Kwon et al., 2005) and NFATc1 (Ishiyama et al., 2015) expression in osteoclast precursors. Downregulation of PU.1 mRNA by CDK8/19 inhibition suggests PU.1 to be a target for CDK8/19 inhibitors upstream of RANK signaling in osteoclast precursors. CDK8/19 inhibition is also reported to prevent elongation of NFκB-induced transcription (Chen et al., 2017). NFκB was detected to be downregulated at 48 hours by Senexin B and

15w. NFATc1, acting downstream of NFκB, induces expression of several genes promoting osteoclast differentiation and function including DC-STAMP, TRAP and cathepsin K (Boyce et al., 2015; Ono and Nakashima, 2018; Takatsuna et al., 2005). By inhibition of CDK8, we detected downregulated NFATc1, DC-STAMP, TRAP and cathepsin K mRNA at 48 hours. Decreased NFATc1 protein levels by CDK8 inhibition confirms NFκB-NFATc1 signaling to be a target of the CDK8/19 inhibitors in osteoclast precursors. In support of an effect on the early stages of osteoclast differentiation was the augmented response to CDK8 inhibition observed on osteoclast numbers and resorption parameters in the 0-48-hour interval. These together with decreased TRAP activity and CTX-I levels in culture supernatant and decreased resorbed area on bone slices confirm that inhibition of CDK8/19 suppresses RANKL-induced osteoclast differentiation.

NFATc1 (Li et al., 2016) and DC-STAMP (Zeng et al., 2015) have been associated with cell cycle progression in cancer cells; however, our findings do not support a similar effect after CDK8 inhibition in BMMs. It is suggested that modulatory effects of cyclin-dependent kinase inhibitors on osteoclast differentiation are not likely to be limited to regulating the switch between proliferation and differentiation (Okahashi et al., 2001; Sankar et al., 2004). Our findings suggest that RANK signaling and its downstream effectors, including NFκB and NFATc1, are targeted by CDK8/19 inhibitors resulting in suppression of osteoclastogenesis.

Although CDK8 activity is reported to be essential for Wnt signaling activation in colorectal cancer cells (Firestein et al., 2008), we found that β-catenin mRNA was upregulated by the CDK8/19 inhibitors in BMMs at 8 and 48 hours. Canonical Wnt/β-catenin signaling inhibits osteoclast differentiation (Weivoda et al., 2015) where overexpression of β-catenin is shown to inhibit osteoclast differentiation (Modarresi et al., 2009). Our data does not exclude a role for canonical Wnt/β-catenin signaling in suppression of osteoclastogenesis mediated by CDK8 inhibition.

Stat1 is reported to have inhibitory effects on osteoclast differentiation (Ivashkiv and Hu, 2004; Lee and Kim, 2011). Similarly, Stat5 acts against osteoclast formation (Lee et al., 2016). Stat1 mRNA levels did not show any significant changes in BMMs after CDK8 inhibition; and Stat5a and Stat5b mRNA expression were downregulated at 48 hours. These data indicate that the inhibitory effect of CDK8 inhibitors on osteoclast differentiation in our study are not mediated through Stat1 or Stat5.

Recent data show that inhibition of CDK8 can have both stimulatory or suppressive effects on osteoblasts and bone formation. CDK8/19 inhibitors, at low doses, are reported to increase procollagen type 1 N-terminal propeptide (P1NP) levels while with higher doses the opposite effect was observed. On the other hand, dose-dependent decreased calcium deposition in murine pre-osteoblastic cell lines, as well as adverse effects on rat bone tissue including dysplasia of growth plate and decreased proliferative zone following systemic treatment with CDK8/19 inhibitors have also been reported (Clarke et al., 2016). In this study, by inhibition of CDK8/19, we observed stimulatory effects on ALP activity and calcium deposition by mouse primary osteoblasts.

Effects of CDK8/19 inhibition on proliferation are highly cell-specific and context-related. There are reports where inhibiting CDK8/19 decreased proliferation (McDermott et al., 2017; Pelish et al., 2015), or increased proliferation (Donner et al., 2007; Gu et al., 2013), or had no effects on proliferation (Crown, 2017; Porter et al., 2012). We did not detect any differences induced by CDK8/19 inhibition in proliferation rate of osteoblasts. Similarly, mRNA levels of p21 and p27, inducers of cell cycle arrest, were not regulated by the inhibitors in osteoblasts. Canonical Wnt/β-catenin signaling promotes osteoblast differentiation, with Runx2 as the main target gene (Baron and Kneissel, 2013). We did not detect significant changes in mRNA expression of β-catenin in osteoblasts. Similarly, Runx2 and its downstream target Osterix (Komori, 2018), showed no significant differences compared to

controls. Neither were any changes detected in mRNA expression of ALP and Col1a1, markers for osteoblast differentiation, as well as bone sialoprotein, which is directly regulated by Osterix (Yang et al., 2016). The RANKL-OPG system was not affected in osteoblasts either as mRNA ratio of RANKL/OPG was not regulated by CDK8/19 inhibition. These data indicate that inhibition of CDK8 exerted no major effects on differentiation of osteoblasts.

CDK8 inhibition is shown to inhibit phosphorylation of Stat1 at Serine 727 (Rzymski et al., 2017). This in turn is reported to increase transcriptional activity of Stat1 (Huang et al., 2016). Although Stat1 (S727) is a known substrate for CDK8, in this study we did not detect any changes in phosphorylation of Stat1 (S727) in osteoblasts suggesting that phosphorylation of Stat1 (S727) does not bear significance for effects of CDK8 inhibition on osteoblasts. On the other hand, both mRNA and protein levels of total Stat1 were decreased after 72 hours by the CDK8/19 inhibitors. Stat1 suppresses osteoblast differentiation (Tajima et al., 2010). $Stat1^{-/-}$ mice have high bone mass despite excessive osteoclastogenesis. Osteoblasts isolated from these mice show elevated differentiation in vitro. It is further demonstrated that Stat1 in its latent form impairs nuclear translocation of Runx2, hence inhibiting its transcriptional activity (Kim et al., 2003). The downregulation of Stat1 by the CDK8/19 inhibitors in this study, could potentially enhance osteoblast differentiation despite total Runx2 expression levels remaining unchanged. Stat5 is reported to support osteoblast differentiation through interaction with Runx2 (Dieudonne et al., 2013). We detected downregulated mRNA levels of Stat5a and Stat5b at 72 hours. Therefore, Stat5 is not likely to mediate effects of CDK8 inhibition on osteoblasts in our study.

Osteopontin is a negative regulator of bone mineralization (Addison et al., 2007; Holm et al., 2014). Furthermore, ALP, which is mainly recognized as a marker for osteoblast differentiation, plays crucial role in mineralization by hydrolyzing inorganic pyrophosphate (PPi), a potent inhibitor of mineralization (Millan, 2013). We detected significant

downregulation of osteopontin mRNA expression by both CDK8/19 inhibitors at 72 hours. Although the increase in ALP mRNA was not statistically significant at 72 hours, the enzyme activity was enhanced at day 10 by Senexin B. This could possibly be explained by post-translational modifications such as shedding from the cell membrane. Downregulation of osteopontin mRNA together with increased ALP activity and calcium deposition demonstrate that inhibition of CDK8 promotes mineralization by mouse primary osteoblasts. Taken together, these data suggest that inhibition of CDK8 has a more prominent effect on osteoblast function rather than on their differentiation or proliferation.

Although 15w appears to be more potent in suppressing osteoclastogenesis and promoting mineralization compared to Senexin B, in vivo activity has only been documented for Senexin B, a well-characterized and readily available inhibitor of CDK8/19 under investigation for other indications as well (McDermott et al., 2017; Ono et al., 2017; Porter et al., 2012; Rzymski et al., 2015). To confirm effects of CDK8 inhibition on bone tissue in vivo, we locally administered Senexin B to bone tissue in a rat model with a drill hole defect on proximal tibiae. A 1-µg dose of Senexin B resulted in increased BV/TV and BMD in the drill hole defect after 14 days compared to controls. Our primary goal was to validate potential in vivo effects through local administration of a CDK8 inhibitor. We were able to show that Senexin B induced enhanced bone regeneration.

CDK19, the paralog of CDK8, is not as well-studied as CDK8. Overlapping but also nonredundant roles for them are suggested (Audetat et al., 2017). Senexin B and 15w are CDK8/19 dual inhibitors; therefore, we cannot conclusively attribute our observations solely to inhibition of CDK8.

Withdrawing CDK8 inhibitors from osteoclast culture showed that the suppression in osteoclastogenesis was not reversible when treatment was stopped and a single-dose regimen

of Senexin B and 15w was capable of suppressing osteoclast differentiation. Similarly, local treatment with a single-dose of Senexin B led to increased BV/TV and BMD in rat tibiae. These indicate CDK8 inhibitors to be promising bone therapeutic agents for local administration. However, the choice of vehicle and dose of CDK8 inhibitors for local effects on bone requires optimization. In summary, our data show that inhibition of CDK8 suppresses osteoclastogenesis and promotes function of osteoblasts. Local administration of such compounds could be used to restrain ongoing osteolysis, promote osseointegration of orthopedic implants, or improve fracture healing. Moreover, with RANK as a target, CDK8/19 inhibitors hold potential to be further investigated as a treatment for systemic resorption disorders or for osteolytic metastasis in cancer patients.

Acknowledgments

This study was supported by Swedish Research Council (Grant numbers: 521-2013-2593, 2016-01822, 2016-06097, K2015-99x-10363-23-4). We thank the late Professor Per Aspenberg for valuable discussions and Angelina Littholt for technical assistance.

Author contributions

MA, GA, JF and AF conceived and designed the study. MA, MB and PL implemented the experiments and analyzed the data. All authors contributed to writing the manuscript. MA, GA, JF and AF revised the manuscript.

Conflict of interest

The authors have no conflicts of interest, financial or otherwise.

References

Addison WN, Azari F, Sorensen ES, Kaartinen MT, Mckee MD. 2007. Pyrophosphate inhibits mineralization of osteoblast cultures by binding to mineral, up-regulating osteopontin, and inhibiting alkaline phosphatase activity. Journal of Biological Chemistry 282(21):15872-15883.

Alarcon C, Zaromytidou AI, Xi Q, Gao S, Yu J, Fujisawa S, Barlas A, Miller AN, Manova-Todorova K, Macias MJ, Sapkota G, Pan D, Massague J. 2009. Nuclear CDKs drive Smad transcriptional activation and turnover in BMP and TGF-beta pathways. Cell 139(4):757-769.

Amend SR, Valkenburg KC, Pienta KJ. 2016. Murine Hind Limb Long Bone Dissection and Bone Marrow Isolation. J Vis Exp(110).

Audetat KA, Galbraith MD, Odell AT, Lee T, Pandey A, Espinosa JM, Dowell RD, Taatjes DJ. 2017. A Kinase-Independent Role for Cyclin-Dependent Kinase 19 in p53 Response. Mol Cell Biol 37(13).

Bakker AD, Klein-Nulend J. 2012. Osteoblast isolation from murine calvaria and long bones. Methods Mol Biol 816:19-29.

Baron R, Kneissel M. 2013. WNT signaling in bone homeostasis and disease: from human mutations to treatments. Nat Med 19(2):179-192.

Bernhardsson M, Sandberg O, Aspenberg P. 2015. Experimental models for cancellous bone healing in the rat. Acta orthopaedica 86(6):745-750.

Bharti AC, Takada Y, Shishodia S, Aggarwal BB. 2004. Evidence that receptor activator of nuclear factor (NF)-kappa B ligand can suppress cell proliferation and induce apoptosis through activation of a NF-kappa B-independent and TRAF6-dependent mechanism. Journal of Biological Chemistry 279(7):6065-6076.

Boyce BF, Xiu Y, Li JB, Xing LP, Yao ZQ. 2015. NF-kappa B-Mediated Regulation of Osteoclastogenesis. Endocrinol Metab-Enm 30(1):35-44.

Chen M, Liang J, Ji H, Yang Z, Altilia S, Hu B, Schronce A, McDermott MSJ, Schools GP, Lim CU, Oliver D, Shtutman MS, Lu T, Stark GR, Porter DC, Broude EV, Roninson IB. 2017. CDK8/19 Mediator kinases potentiate induction of transcription by NFkappaB. Proc Natl Acad Sci U S A 114(38):10208-10213.

Clarke PA, Ortiz-Ruiz MJ, TePoele R, Adeniji-Popoola O, Box G, Court W, Czasch S, El Bawab S, Esdar C, Ewan K, Gowan S, De Haven Brandon A, Hewitt P, Hobbs SM, Kaufmann W, Mallinger A, Raynaud F, Roe T, Rohdich F, Schiemann K, Simon S, Schneider R, Valenti M, Weigt S, Blagg J, Blaukat A, Dale TC, Eccles SA, Hecht S, Urbahns K, Workman P, Wienke D. 2016. Assessing the mechanism and therapeutic potential of modulators of the human Mediator complex-associated protein kinases. Elife 5.

Crown J. 2017. CDK8: a new breast cancer target. Oncotarget 8(9):14269-+.

Dieudonne FX, Severe N, Biosse-Duplan M, Weng JJ, Su Y, Marie PJ. 2013. Promotion of Osteoblast Differentiation in Mesenchymal Cells Through Cbl-Mediated Control of STAT5 Activity. Stem Cells 31(7):1340-1349.

Donner AJ, Szostek S, Hoover JM, Espinosa JM. 2007. CDK8 is a stimulus-specific positive coregulator of p53 target genes. Mol Cell 27(1):121-133.

Firestein R, Bass AJ, Kim SY, Dunn IF, Silver SJ, Guney I, Freed E, Ligon AH, Vena N, Ogino S, Chheda MG, Tamayo P, Finn S, Shrestha Y, Boehm JS, Jain S, Bojarski E, Mermel C, Barretina J, Chan JA, Baselga J, Tabernero J, Root DE, Fuchs CS, Loda M, Shivdasani RA,

Meyerson M, Hahn WC. 2008. CDK8 is a colorectal cancer oncogene that regulates beta-catenin activity. Nature 455(7212):547-551.
Fryer CJ, White JB, Jones KA. 2004. Mastermind recruits CycC:CDK8 to phosphorylate the Notch ICD and coordinate activation with turnover. Mol Cell 16(4):509-520.
Galbraith MD, Donner AJ, Espinosa JM. 2010. CDK8: a positive regulator of transcription. Transcription 1(1):4-12.
Gu WT, Wang CG, Li WH, Hsu FN, Tian LF, Zhou J, Yuan CZ, Xie XJ, Jiang T, Addya S, Tai YH, Kong BH, Ji JY. 2013. Tumor-suppressive effects of CDK8 in endometrial cancer cells. Cell Cycle 12(6):987-999.
Haarhaus M, Arnqvist HJ, Magnusson P. 2013. Calcifying Human Aortic Smooth Muscle Cells Express Different Bone Alkaline Phosphatase Isoforms, Including the Novel B1x Isoform. J Vasc Res 50(2):167-174.
Herchenhan A, Bayer ML, Eliasson P, Magnusson SP, Kjaer M. 2015. Insulin-like growth factor I enhances collagen synthesis in engineered human tendon tissue. Growth Horm IGF Res 25(1):13-19.
Holm E, Gleberzon JS, Liao YY, Sorensen ES, Beier F, Hunter GK, Goldberg HA. 2014. Osteopontin mediates mineralization and not osteogenic cell development in vitro. Biochemical Journal 464:355-364.
Huang B, Wang WH, Li QC, Wang ZY, Yan B, Zhang ZM, Wang L, Huang MJ, Jia CH, Lu JS, Liu SC, Chen HD, Li MM, Cai DZ, Jiang Y, Jin DD, Bai XC. 2016. Osteoblasts secrete Cxcl9 to regulate angiogenesis in bone. Nat Commun 7.
Ishiyama K, Yashiro T, Nakano N, Kasakura K, Miura R, Hara M, Kawai F, Maeda K, Tamura N, Okumura K, Ogawa H, Takasaki Y, Nishiyama C. 2015. Involvement of PU.1 in NFATc1 promoter function in osteoclast development. Allergol Int 64(3):241-247.
Ivashkiv LB, Hu XY. 2004. Signaling by STATs. Arthritis Res Ther 6(4):159-168.
Kim HJ, Zou W, Ito Y, Kim SY, Chappel J, Ross FP, Teitelbaum SL. 2010. Src-like adaptor protein regulates osteoclast generation and survival. J Cell Biochem 110(1):201-209.
Kim S, Koga T, Isobe M, Kern BE, Yokochi T, Chin YE, Karsenty G, Taniguchi T, Takayanagi H. 2003. Stat1 functions as a cytoplasmic attenuator of Runx2 in the transcriptional program of osteoblast differentiation. Genes Dev 17(16):1979-1991.
Komori T. 2018. Runx2, an inducer of osteoblast and chondrocyte differentiation. Histochem Cell Biol.
Kwon M, Kim JM, Lee K, Park SY, Lim HS, Kim T, Jeong D. 2016. Synchronized Cell Cycle Arrest Promotes Osteoclast Differentiation. Int J Mol Sci 17(8).
Kwon OH, Lee CK, Lee YI, Paik SG, Lee HJ. 2005. The hematopoietic transcription factor PU.1 regulates RANK gene expression in myeloid progenitors. Biochem Biophys Res Commun 335(2):437-446.
Lång P, Andersson G. 2005. Differential expression of monomeric and proteolytically processed forms of tartrate-resistant acid phosphatase in rat tissues. Cell Mol Life Sci 62(7-8):905-918.
Law ME, Corsino PE, Narayan S, Law BK. 2015. Cyclin-Dependent Kinase Inhibitors as Anticancer Therapeutics. Mol Pharmacol 88(5):846-852.
Lee J, Seong S, Kim JH, Kim K, Kim I, Jeong BC, Nam KI, Kim KK, Hennighausen L, Kim N. 2016. STAT5 is a key transcription factor for IL-3-mediated inhibition of RANKL-induced osteoclastogenesis. Sci Rep-Uk 6.
Lee Y, Kim HH. 2011. The Role of Jak/STAT Pathways in Osteoclast Differentiation. Biomol Ther 19(2):141-148.
Li L, Duan Z, Yu J, Dang HX. 2016. NFATc1 regulates cell proliferation, migration, and invasion of ovarian cancer SKOV3 cells in vitro and in vivo. Oncol Rep 36(2):918-928.
McDermott MSJ, Chumanevich AA, Lim CU, Liang JX, Chen MQ, Altilia S, Oliver D, Rae JM, Shtutman M, Kiaris H, Gyorffy B, Roninson IB, Broude EV. 2017. Inhibition of CDK8 mediator kinase suppresses estrogen dependent transcription and the growth of estrogen receptor positive breast cancer. Oncotarget 8(8):12558-12575.
Millan JL. 2013. The Role of Phosphatases in the Initiation of Skeletal Mineralization. Calcified Tissue Int 93(4):299-306.

Mizoguchi T, Muto A, Udagawa N, Arai A, Yamashita T, Hosoya A, Ninomiya T, Nakamura H, Yamamoto Y, Kinugawa S, Nakamura M, Nakamichi Y, Kobayashi Y, Nagasawa S, Oda K, Tanaka H, Tagaya M, Penninger JM, Ito M, Takahashi N. 2009. Identification of cell cycle-arrested quiescent osteoclast precursors in vivo. J Cell Biol 184(4):541-554.

Modarresi R, Xiang ZY, Yin M, Laurence J. 2009. WNT/beta-Catenin Signaling Is Involved in Regulation of Osteoclast Differentiation by Human Immunodeficiency Virus Protease Inhibitor Ritonavir Relationship to Human Immunodeficiency Virus-Linked Bone Mineral Loss. American Journal of Pathology 174(1):123-135.

Morris EJ, Ji JY, Yang F, Di Stefano L, Herr A, Moon NS, Kwon EJ, Haigis KM, Naar AM, Dyson NJ. 2008. E2F1 represses beta-catenin transcription and is antagonized by both pRB and CDK8. Nature 455(7212):552-556.

Nemet J, Jelicic B, Rubelj I, Sopta M. 2014. The two faces of Cdk8, a positive/negative regulator of transcription. Biochimie 97:22-27.

Okahashi N, Murase Y, Koseki T, Sato T, Yamato K, Nishihara T. 2001. Osteoclast differentiation is associated with transient upregulation of cyclin-dependent kinase inhibitors p21(WAF1/CIP1) and p27(KIP1). J Cell Biochem 80(3):339-345.

Ono K, Banno H, Okaniwa M, Hirayama T, Iwamura N, Hikichi Y, Murai S, Hasegawa M, Hasegawa Y, Yonemori K, Hata A, Aoyama K, Cary DR. 2017. Design and synthesis of selective CDK8/19 dual inhibitors: Discovery of 4,5-dihydrothieno[3',4':3,4]benzo[1,2-d]isothiazole derivatives. Bioorg Med Chem 25(8):2336-2350.

Ono T, Nakashima T. 2018. Recent advances in osteoclast biology. Histochem Cell Biol.

Patlaka C, Norgard M, Paulie S, Nordvall-Bodell A, Lang P, Andersson G. 2014. Caveolae-mediated endocytosis of the glucosaminoglycan-interacting adipokine tartrate resistant acid phosphatase 5a in adipocyte progenitor lineage cells. Biochim Biophys Acta 1843(3):495-507.

Pelish HE, Liau BB, Nitulescu II, Tangpeerachaikul A, Poss ZC, Da Silva DH, Caruso BT, Arefolov A, Fadeyi O, Christie AL, Du K, Banka D, Schneider EV, Jestel A, Zou G, Si C, Ebmeier CC, Bronson RT, Krivtsov AV, Myers AG, Kohl NE, Kung AL, Armstrong SA, Lemieux ME, Taatjes DJ, Shair MD. 2015. Mediator kinase inhibition further activates super-enhancer-associated genes in AML. Nature 526(7572):273-+.

Porter DC, Farmaki E, Altilia S, Schools GP, West DK, Chen M, Chang BD, Puzyrev AT, Lim CU, Rokow-Kittell R, Friedhoff LT, Papavassiliou AG, Kalurupalle S, Hurteau G, Shi J, Baran PS, Gyorffy B, Wentland MP, Broude EV, Kiaris H, Roninson IB. 2012. Cyclin-dependent kinase 8 mediates chemotherapy-induced tumor-promoting paracrine activities. Proc Natl Acad Sci U S A 109(34):13799-13804.

Poss ZC, Ebmeier CC, Odell AT, Tangpeerachaikul A, Lee T, Pelish HE, Shair MD, Dowell RD, Old WM, Taatjes DJ. 2016. Identification of Mediator Kinase Substrates in Human Cells using Cortistatin A and Quantitative Phosphoproteomics. Cell Reports 15(2):436-450.

Reno C, Marchuk L, Sciore P, Frank CB, Hart DA. 1997. Rapid isolation of total RNA from small samples of hypocellular, dense connective tissues. Biotechniques 22(6):1082-1086.

Ronnison IBL, SC, US), Porter, Donald C. (Columbia, SC, US), Wentland, Mark P. (Watervilet, NY, US); SENEX BIOTECHNOLOGY INC. (Columbia, SC, US), assignee. 2014. CDK8-CDK19 selective inhibitors and their use in anti-metastatic and chemopreventative methods for cancer. United States.

Rzymski T, Mikula M, Wiklik K, Brzozka K. 2015. CDK8 kinase-An emerging target in targeted cancer therapy. Bba-Proteins Proteom 1854(10):1617-1629.

Rzymski T, Mikula M, Zylkiewicz E, Dreas A, Wiklik K, Golas A, Wojcik K, Masiejczyk M, Wrobel A, Dolata I, Kitlinska A, Statkiewicz M, Kuklinska U, Goryca K, Sapala L, Grochowska A, Cabaj A, Szajewska-Skuta M, Gabor-Worwa E, Kucwaj K, Bialas A, Radzimierski A, Combik M, Woyciechowski J, Mikulski M, Windak R, Ostrowski J, Brzozka K. 2017. SEL120-34A is a novel CDK8 inhibitor active in AML cells with high levels of serine phosphorylation of STAT1 and STAT5 transactivation domains. Oncotarget 8(20):33779-33795.

Sankar U, Patel K, Rosol TJ, Ostrowski MC. 2004. RANKL coordinates cell cycle withdrawal and differentiation in osteoclasts through the cyclin-dependent kinase inhibitors p27(KIP1) and p21(CIP1). Journal of Bone and Mineral Research 19(8):1339-1348.

Szilagyi Z, Gustafsson CM. 2013. Emerging roles of Cdk8 in cell cycle control. Biochim Biophys Acta 1829(9):916-920.

Tajima K, Takaishi H, Takito J, Tohmonda T, Yoda M, Ota N, Kosaki N, Matsumoto M, Ikegami H, Nakamura T, Kimura T, Okada Y, Horiuchi K, Chiba K, Toyama Y. 2010. Inhibition of STAT1 Accelerates Bone Fracture Healing. J Orthopaed Res 28(7):937-941.

Takatsuna H, Asagiri M, Kubota T, Oka K, Osada T, Sugiyama C, Saito H, Aoki K, Ohya K, Takayanagi H, Umezawa K. 2005. Inhibition of RANKL-induced osteoclastogenesis by (-)-DHMEQ, a novel NF-kappaB inhibitor, through downregulation of NFATc1. Journal of bone and mineral research : the official journal of the American Society for Bone and Mineral Research 20(4):653-662.

Vidal A, Koff A. 2000. Cell-cycle inhibitors: three families united by a common cause. Gene 247(1-2):1-15.

Watanabe K, Tominari T, Hirata M, Matsumoto C, Hirata J, Murphy G, Nagase H, Miyaura C, Inada M. 2017. Indoxyl sulfate, a uremic toxin in chronic kidney disease, suppresses both bone formation and bone resorption. Febs Open Bio 7(8):1178-1185.

Weivoda MM, Ruan M, Hachfeld CM, Pederson L, Howe A, Davey RA, Zajac JD, Kobayashi Y, Williams BO, Westendorf JJ, Khosla S, Oursler MJ. 2015. Wnt Signaling Inhibits Osteoclast Differentiation by Activating Canonical and Noncanonical cAMP/PKA Pathways. Journal of bone and mineral research : the official journal of the American Society for Bone and Mineral Research.

Wermelin K, Suska F, Tengvall P, Thomsen P, Aspenberg P. 2008. Stainless steel screws coated with bisphosphonates gave stronger fixation and more surrounding bone. Histomorphometry in rats. Bone 42(2):365-371.

Yang Y, Huang YH, Zhang L, Zhang C. 2016. Transcriptional regulation of bone sialoprotein gene expression by Osx. Biochem Bioph Res Co 476(4):574-579.

Zeng XX, Chu TJ, Yuan JY, Zhang W, Du YM, Ban ZY, Lei DM, Cao J, Zhang Z. 2015. Transmembrane 7 superfamily member 4 regulates cell cycle progression in breast cancer cells. Eur Rev Med Pharmacol Sci 19(22):4353-4361.

Figures

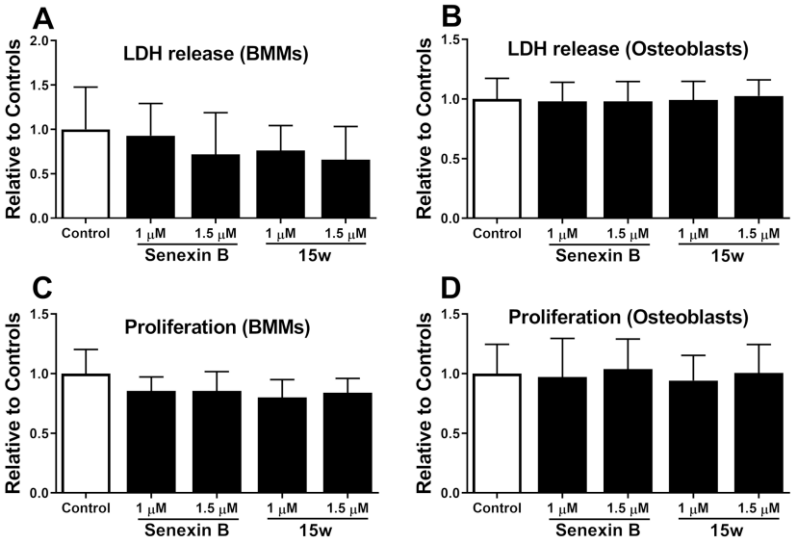

Figure 1. CDK8/19 inhibitors displayed no effects on LDH release or cell proliferation. There was no difference in lactate dehydrogenase (LDH) release rate from (**A**) mouse BMMs (n = 6) or (**B**) osteoblasts (n = 6) after treatment with 1 and 1.5 µM of the CDK8/19 inhibitors for 24 hours compared to controls. Proliferation rate of (**C**) mouse BMMs (n = 6) and (**D**) osteoblasts (n = 6) did not show any differences compared to controls after treatment with 1 and 1.5 µM of the CDK8/19 inhibitors for 8 hours. Results are presented as mean ± SD.

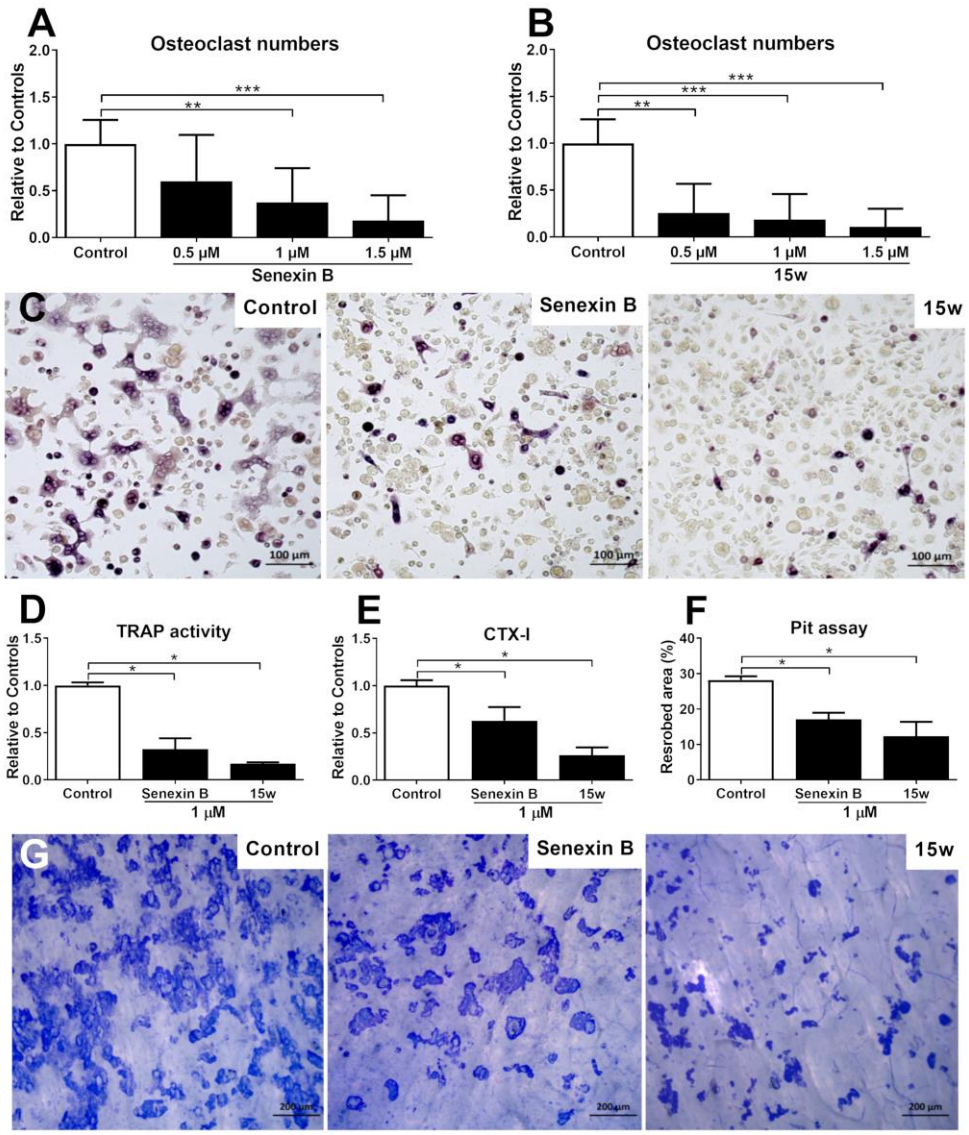

Figure 2. Osteoclast differentiation was suppressed by CDK8/19 inhibitors. RANKL-induced osteoclast differentiation from mouse (n = 7) BMMs was suppressed by (**A**) Senexin B, and (**B**) 15w. (**C**) Representative images of TRAP-positive multinucleated osteoclasts on day 4 after treatment with CDK8/19 inhibitors (1.5 μM). Scale bar indicates 100 μm. CDK8/19 inhibitors at 1 μM decreased (**D**) TRAP activity and (**E**) CTX-I levels in culture supernatant from days 10-12, and (**F**, **G**) the resorbed area on bovine bone slices on day 12 (n = 3). Scale bar indicates 200 μm. Results are presented as mean ± SD. *: p-value ≤ 0.05; **: p-value ≤ 0.01; ***: p-value ≤ 0.001.

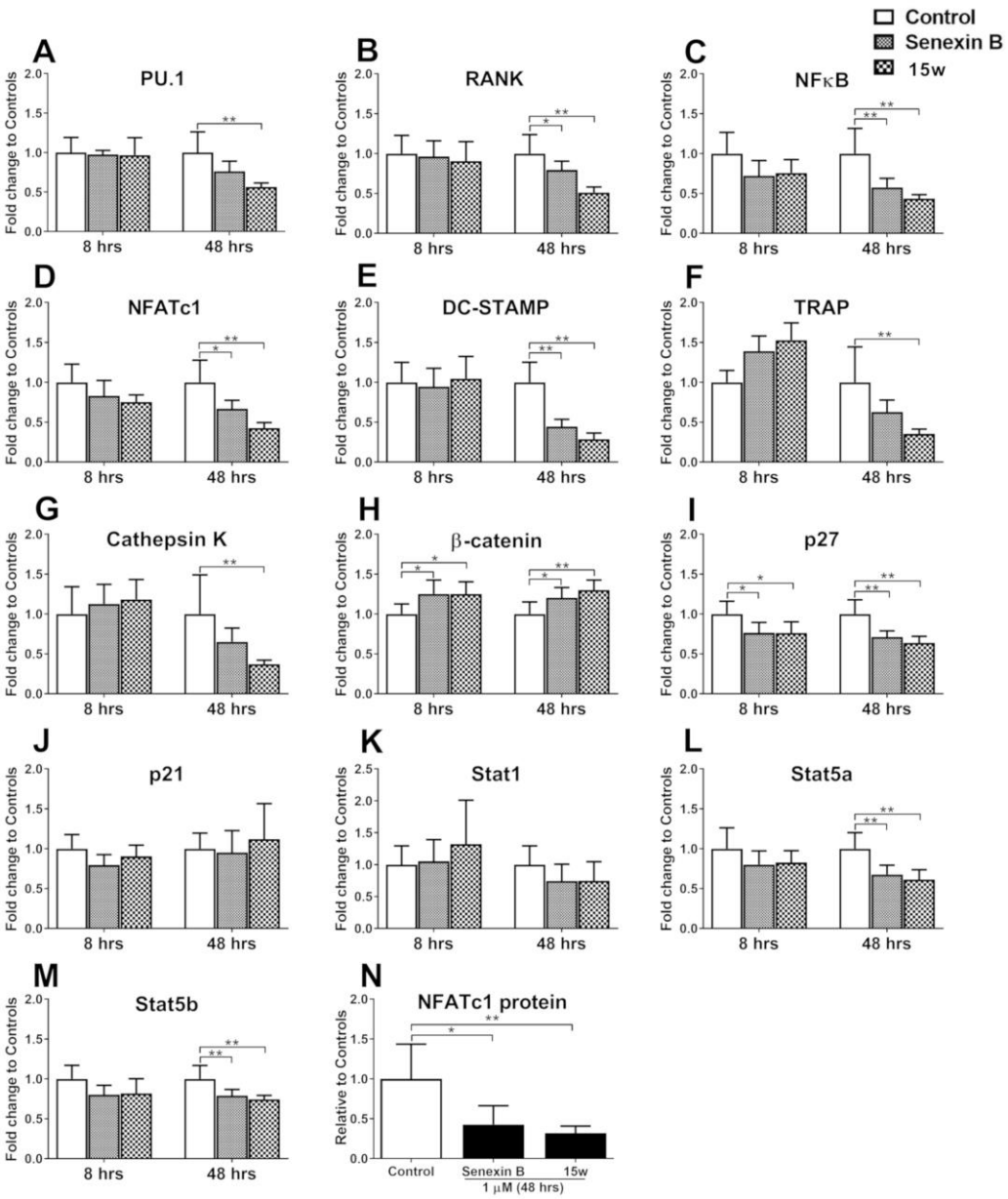

Figure 3. CDK8/19 inhibition suppressed expression for osteoclastogenesis-related genes as well as protein levels of NFATc1 in RANKL-stimulated bone marrow macrophages (BMMs). Mouse (n = 6) BMMs were treated with 1 μM of Senexin B and 15w for 8 and 48 hours. mRNA expression changes were investigated by qPCR. Gene expression levels were normalized to geometric mean of beta-actin and beta-2 microglobulin. Results are presented as mean ± SD. *: p-value ≤ 0.05; **: p-value ≤ 0.01.

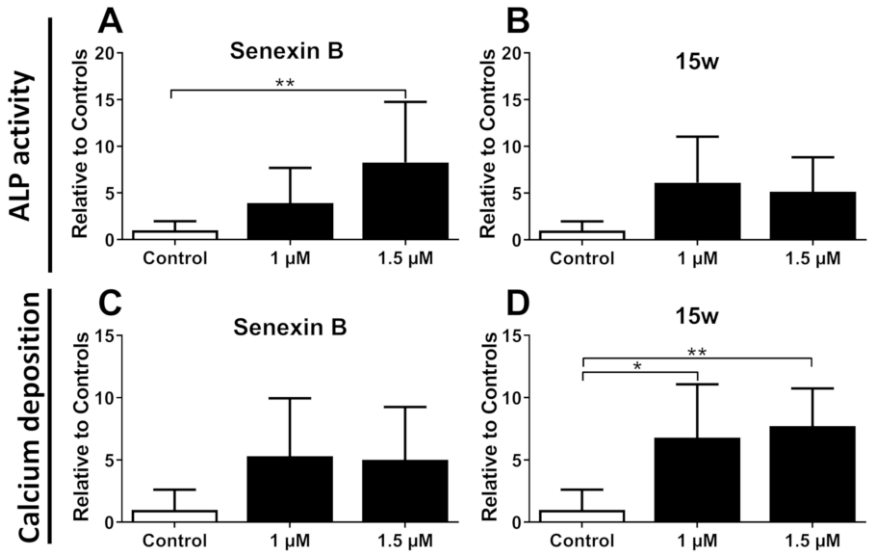

Figure 4. Alkaline phosphatase (ALP) activity and calcium deposition in primary osteoblasts were increased by CDK8/19 inhibition. CDK8/19 inhibition increased (**A**, **B**) ALP activity at day 10, and (**C**, **D**) calcium deposition at day 18 in mouse (n = 5) primary osteoblasts. Results are presented as mean ± SD. *: p-value ≤ 0.05; **: p-value ≤ 0.01.

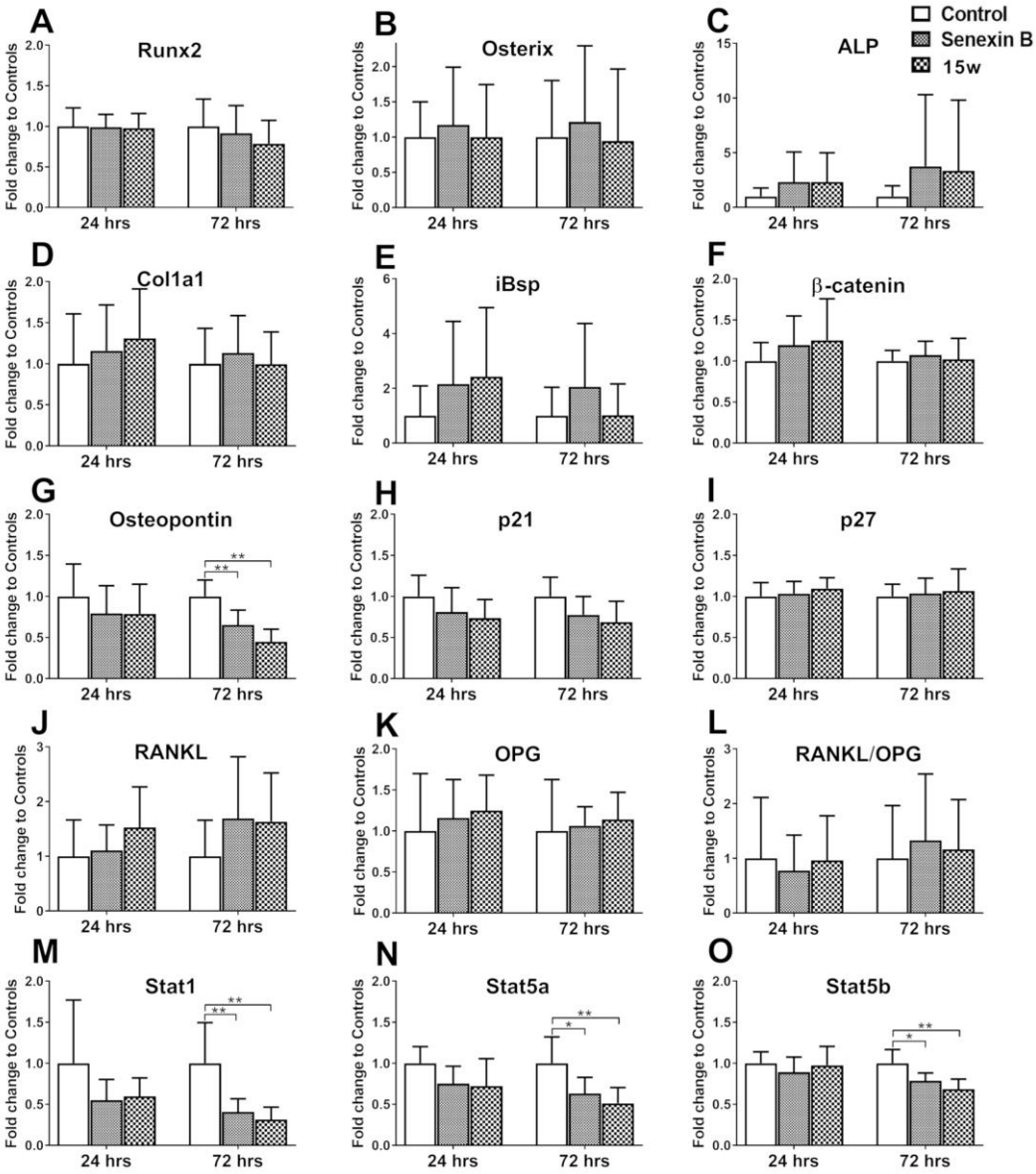

Figure 5. Inhibition of CDK8/19 did not regulate mRNA levels of osteoblast differentiation markers while osteopontin was downregulated. Mouse (n = 6) primary osteoblasts were treated with 1 μM of Senexin B and 15w for 24 and 72 hours. mRNA expression changes were investigated by qPCR. Gene expression levels in osteoblasts were normalized to beta-actin levels. Results are presented as mean ± SD. *: p-value ≤ 0.05; **: p-value ≤ 0.01.

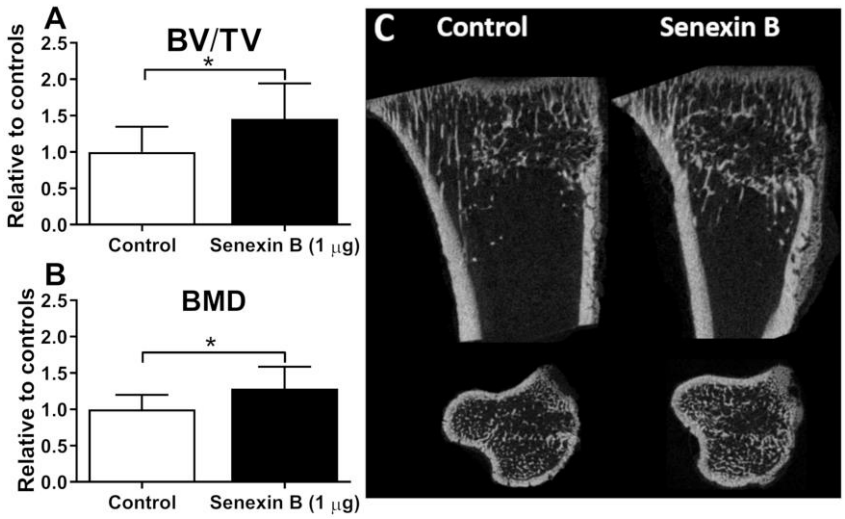

Figure 6. Effects of local treatment with a CDK8/19 inhibitor on bone regeneration in a drill hole defect on rat tibiae. Micro-CT analysis of rat tibiae 14 days after local administration of 1 µg of Senexin B into the drill holes showed (**A**) increased bone volume fraction (BV/TV) and (**B**) bone mineral density (BMD) compared to controls (n = 15/group). (**C**) Representative micro-CT scans chosen based on BV/TV median. Results are presented as mean ± SD.*: p-value ≤ 0.05.

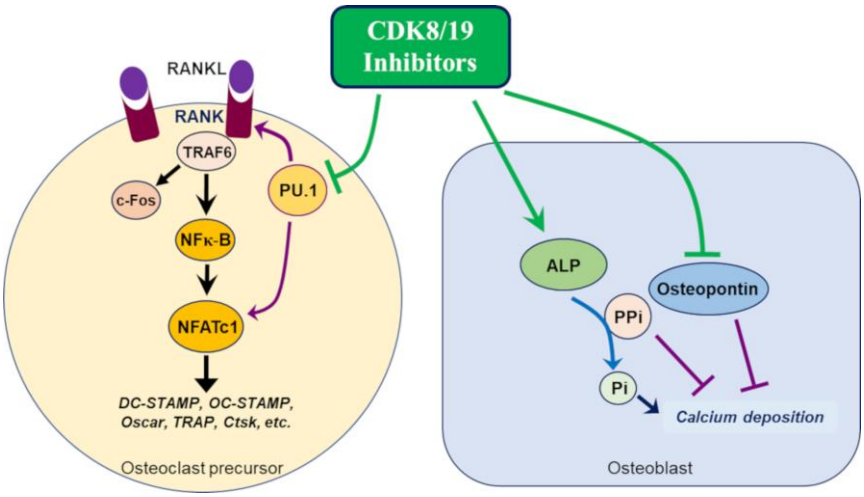

Figure 7. Inhibition of CDK8/19 suppressed RANKL-induced osteoclastogenesis through disruption of RANK signaling in osteoclast precursors and promoted osteoblast mineralization by enhanced alkaline phosphatase (ALP) activity and downregulation of osteopontin.